HHS Public Access

Author manuscript

Science. Author manuscript; available in PMC 2019 May 21.

Published in final edited form as:

Science. 2012 May 18; 336(6083): 925–931. doi:10.1126/science.1215317.

Multiple Spectral Inputs Improve Motion Discrimination in the Drosophila Visual System

Trevor J. Wardill[1,*], **Olivier List**[1,*], **Xiaofeng Li**[1,2,*], **Sidhartha Dongre**[1], **Marie McCulloch**[1], **Chun-Yuan Ting**[3], **Cahir J. O'Kane**[4], **Shiming Tang**[2], **Chi-Hon Lee**[3], **Roger C. Hardie**[5], and **Mikko Juusola**[1,2,†]

[1]Department of Biomedical Science, University of Sheffield, Sheffield S10 2TN, UK.

[2]State Key Laboratory of Cognitive Neuroscience and Learning, Beijing Normal University, Beijing 100875, China.

[3]Eunice Kennedy Shriver National Institute of Child Health and Human Development, National Institutes of Health, Bethesda, MD 20892–5431, USA.

[4]Department of Genetics, University of Cambridge, Cambridge CB2 3EH, UK.

[5]Department of Physiology, Development and Neuroscience, University of Cambridge, Cambridge CB3 2EG, UK.

Abstract

Color and motion information are thought to be channeled through separate neural pathways, but it remains unclear whether and how these pathways interact to improve motion perception. In insects, such as Drosophila, it has long been believed that motion information is fed exclusively by one spectral class of photoreceptor, so-called R1 to R6 cells; whereas R7 and R8 photoreceptors, which exist in multiple spectral classes, subserve color vision. Here, we report that R7 and R8 also contribute to the motion pathway. By using electrophysiological, optical, and behavioral assays, we found that R7/R8 information converge with and shape the motion pathway output, explaining flies' broadly tuned optomotor behavior by its composite responses. Our results demonstrate that inputs from photoreceptors of different spectral sensitivities improve motion discrimination, increasing robustness of perception.

The integration of color and motion signals at the neural circuit level is poorly understood, but combining these inputs is thought to improve perceptual discrimination (1, 2), reducing uncertainty to make judgments and guide actions in the world (3, 4). However, it remains elusive to what extent information from different spectral channels (5, 6) is exploited to improve motion detection and orienting behavior (7–10). The modular architecture of the Drosophila visual system, with its genetic malleability and accessibility to in vivo recordings (11–14), makes it a powerful model to study such circuit computations. Its multifaceted

†To whom correspondence should be addressed. m.juusola@sheffield.ac.uk.
*These authors contributed equally to this work.

Supplementary Materials
www.sciencemag.org/cgi/content/full/336/6083/925/DC1
Materials and Methods

compound eyes are composed of ~750 ommatidia, each containing photoreceptor cells with a suite of spectral sensitivities (6, 15, 16). Light from a point in space excites eight photoreceptors, R1 to R8, distributed across seven ommatidia (Fig. 1A) (6). Because each of these photoreceptors innervate either the parallel motion or color pathway, they are thought to subserve specific visual behaviors (17, 18), and for over 30 years most researchers have considered insect motion vision to be mediated exclusively by the single spectral class, R1–R6 (9, 11, 17–20).

Outer photoreceptors R1–R6 (6), expressing blue-green Rh1-opsin (21) and ultraviolet (UV)-sensitizing pigment (22), mediate motion detection (20) by innervating (23) large mono-polar cells (LMCs, L1 and L2) (11, 18) in the first optic neuropile, the lamina. These neurons, which thus should have the same spectral sensitivity as R1–R6, project to the second optic neuropile, the medulla (24). The signals transmit from medulla output layers to the motion-sensitive tangential cells of the lobula plate (LPTCs), feeding the fly's optomotor behavior to changing optic flow fields (25). Light also excites central photoreceptors, R7 and underneath it R8, initiating the color pathway. R7s express UV-sensitive opsins (R7p:Rh3; R7y:Rh4), whereas R8s express blue- (R8p:Rh5) or green-yellow–sensitive opsins (R8y:Rh6), having 30:70 retinal distributions, respectively (6, 16). R7s/R8s innervate separate medulla layers (24), where some contribution to their processing comes from R1–R6 via monopolar neurons L3 (17).

Although motion information appears routed and processed through dedicated on and off channels (11, 26, 27), in principle R1–R6 channels might cross-talk with the color channels in places. Ultrastructural studies imply interactions in the medulla, with synapses between R7/R8 photo-receptors and LMCs (24), but possibly also in the lamina, where gap junctions (28, 29) and synapses (13) form sophisticated local processing networks (30). Here, combining information from different channels could improve the sensitivity, precision, and robustness of their neural messages. However, such interactions are hard to investigate because the spectral sensitivities of the color and motion channels overlap extensively. This interference makes it difficult to activate one pathway without activating the other.

To overcome this problem, we generated flies, referred to as UV flies, in which the R1–R6 blue-green opsin (Rh1, also known as *ninaE*) was mutated [$ninaE^{8}$, also $ninaE^{P334}$ (31)], making it functionally inactive, and a UVopsin (Rh3) (32) was expressed in R1–R6 photoreceptors in its place (Fig. 1B). Mutant $ninaE^{8}$ flies were selected because they have intact R1–R6 ultrastructure (33) while their R7/R8 photoreceptors function normally (Fig. 1F and fig. S2); by contrast, many alternative *ninaE* lines carry additional mutations (fig. S2 and table S1), which may blind them (34). Hence, by using a monochromator light source, R8s of UV flies could now be independently excited by long-wavelength light (≥480 nm), whereas R1–R6s should only respond to short-wavelength light (<480 nm).

Whole-cell recordings of dissociated R1–R6 photoreceptors from these UV flies indicated that, apart from the expected UV sensitivity of Rh3-opsin (Fig. 1C and fig. S3), their phototransduction dynamics (Fig. 1D) approximate those of the wild-type photoreceptors (35). The intact retina ultrastructure (Fig. 1E and fig. S1B), in vivo electroretinograms (Fig. 1F), and response dynamics (fig. S4) indicated undistorted signal transmission from R1–R6

to LMCs, suggesting that the underlying circuit computations were normal. Therefore, by using green-amber stimulation, which is essentially invisible to these UV-sensitive R1–R6s but excites R8 photoreceptors, we could examine whether there is cross-talk between different photoreceptor classes.

Intracellular recordings (Fig. 2A) in R1–R6s and LMCs from UV flies showed that input from R8 photoreceptors can already be detected in the lamina circuits. In addition to their predicted UV sensitivity (Fig. 2B), ~30% of R1–R6 photo-receptors (12/36, putatively axons) and all LMCs (28/28) responded to longer wavelength flashes, either by brief depolarizations (LMCs 7%; Fig. 2C, left and right) or hyperpolarizations (LMCs 93%; Fig. 2C, middle), mapping R8y or R8p photoreceptors' spectral range (Fig. 2D; corresponding nomograms). These relatively small and slightly delayed responses implied that their input probably came through gap junctions or synapses at the level of R1–R6 terminals (fig. S5A) and, in somatic photoreceptor recordings, reflected signal degradation by back propagation. Their opposing polarities confirmed that these signals were neither recording artifacts nor field potentials (fig. S6). Thus, the spectral sensitivity of many R1–R6s and every tested LMC was selectively boosted in the 460- to 600-nm range (Fig. 2D).

These findings support a wiring model (Fig. 2E) in which one photoreceptor (R6 or neighboring R1) receives information from either a R8y or R8p cell, in keeping with results from larger dipteran flies (fig. S7) (28, 29). This input would then spread decrementally between R1–R6 via gap junctions (29, 36), showing diminishing green-yellow sensitivity the farther a recorded photoreceptor is from a R6 in the cartridge (fig. S6A). Because every R1–R6 forms synapses with every L1–L3 (30), all LMCs in the same cartridge should receive this information. Correspondingly, all LMCs showed larger responses to green-yellow than those recorded from R1–R6s (Fig. 2D). Nonetheless, LMCs' responsiveness to long wavelengths (460 to 620 nm) was ~10 times less(9.5% ± 7.0, SD; $n = 28$; range 2.8 to 34.4%) than that to UV light (100%; 300 to 440 nm), consistent with the model that they receive green-yellow inputs mainly from one R6 instead of the normal R1–R6. In some LMC recordings, the speed and size of depolarizations to green-yellow stimuli (Fig. 2, C and E, middle) implied that the R8 axon forms gap junctions with one LMC and that such signals feed back to selected R1–R6s (fig. S5A), inhibiting their output.

To assess the contribution of R7/R8 input to neural signaling between R1–R6 and LMCs, we crossed our UV flies into a phototransduction mutant background ($norpA^{36}$), which rendered all photoreceptors blind, and then rescued only R1–R6 by using a wild-type norpA transgene, resulting in structurally intact but light-insensitive R7/R8 photoreceptors (Fig. 2F). Because this manipulation prevented R7/R8 phototransduction, we could quantify information transfer from the color pathway to R1–R6 and LMCs by compar ing their outputs with and without R7/R8 inputs, but with effectively wild-type R1–R6 dynamics and impedances (fig. S4, C and D). Without R7/R8 inputs, R1–R6s and LMCs could respond only to 300- to 440-nm stimuli (Fig. 2, G to I), following the spectral sensitivity of the UV-opsin expressed in R1–R6 photoreceptors (Fig. 1C). When R7/R8 cells were not participating in the circuit, the responses of R1–R6s were briefer when saturated with a UV impulse (340 ± 20 nm), which maximally excites R1–R6s and R7s but only slightly R8s (Fig. 3A and fig. S5B). The briefer responses of R1–R6s [half-width: $P = 0.009$, oneway

analysis of variance (ANOVA)] and LMCs ($P = 0.021$) as seen over the tested spectral range in recordings probably reflected the lack of R7/R8 input in their processing.

We next quantified how R7/R8 inputs affect encoding of R1–R6s (Fig. 3B) by using repeated stimulation with naturalistic intensity patterns in preparations where R7/R8s either functioned normally or were light-insensitive. With functionally intact R7/R8s, the signal-to-noise ratio of R1–R6 photoreceptors for low-frequency UV stimulation (<10 Hz, 390 nm) was increased by ~100% (Fig. 3C; $P < 0.05$, one-way ANOVA); on average, this equals an extra 10 to 20 bit/s (or ~5 to 10%; inset) on a R1–R6's information transfer (37). However, transfer of long-wavelength (595 nm) information in presumptive R6s (Fig. 3, D and E)—that is, ~12% of R1–R6 photoreceptors, which receive the direct feed from R8y photoreceptors (28, 29) of the color pathway [70% lamina cartridges (16)]—could be as high as 70% compared with that of a similar UV stimulus in the same cells (Fig. 3F), indicating efficient communication between R8 and R6 axons. Thus, R7/R8 inputs boost the amplitude range of relatively slow voltage deflections to capture better the temporal structure of the dominant slow contrast changes in Drosophila's natural environment (38).

We then used *ninaE*^{8} flies to determine whether R7/R8 input alone is sufficient to drive LMC output. In vitro patch-clamp experiments showed no macroscopic light responses in their R1–R6s (Fig. 3G) but essentially normal K^+ conductances (fig. S4F) and only moderately reduced capacitance. In vivo, we struggled to record light-induced voltage responses in the retina from R1–R6 somata. However, their axons closer to (or within) the lamina responded to a broad spectral range of light pulses with small rapidly rising depolarizations (Fig. 3H and fig. S5C), implying that they receive information from R7/R8s (28, 29) through functional contacts, as in UV flies (Fig. 2C and fig. S5A). This information was faithfully transmitted to LMCs, all of which responded to light. Notably, the responses of most R1–R6s (9/11) and all postsynaptic LMCs (9/9) (Fig. 3H) followed the distinctive spectral sensitivity of R7p/R8p or R7y/R8y pairs (Fig. 3I) (6, 15, 16); two R1–R6s were UV-sensitive (fig. S5D). This suggests that presynaptic coupling between R1–R6 and R7/R8 axons can extend neural superposition in most lamina cartridges to eight photoreceptors (instead of the assumed six), further improving information transfer to LMCs (13). We conclude that R7 and R8 inputs alone in ninaE^{8} and UV flies can drive the synaptic output of R1–R6 terminals (Fig. 3J) to activate the on and off channels [L1 and L2 monopolar cells, respectively (11)] for motion detection.

Although these results (Figs. 2 and 3) demonstrate the spectral and temporal push-and-pull of R7/R8s input on both R1–R6 and LMC outputs, supporting a wiring model in which color pathways refine signaling in on and off channels, it remained unclear whether this information is sufficient or necessary for motion perception. To resolve these questions, we next examined *Drosophila's* optomotor behavior.

By using a classic flight simulator system (*18, 20*), we quantified how altering the spectral sensitivity or availability of photoreceptor inputs affect the flies' behavioral responses to colored field rotations. Figure 4 shows the average optomotor responses (yaw torque) of tethered flying wild-type (WT) flies, UV flies, and specific mutants to black-and-white, black-and-blue, or black-and-amber field rotations, which were chosen to evaluate the

relative contribution of R7/R8 photo-receptors to their motion detection (control and individual responses are in figs. S9 and S10).

If all R7s/R8s supplied inputs to the motion pathway, then UV flies should show spectrally broad optomotor behavior. Indeed, their responses to the colored motion stimuli covered the range of WT responses (Fig. 4A), including amber motion, which in UV flies is only visible to their R8y photoreceptors. Naturally, WT R1–R6s could resolve amber motion better, because of their broadly tuned Rh1-opsin (Fig. 1B) and further boosting by R8y input via functional contacts, before transmission to the LMC on and off channels (11, 26). Nonetheless, the overall similar response dynamics of UVand WT flies strongly suggest that the underlying computations in their motion-detection and flight-control circuits are similar (Fig. 4A, left).

Because input from R7/R8s alone can drive the synaptic terminals of otherwise light-insensitive R1–R6s (Fig. 3, H and I), our model predicts that *ninaE*^{8} flies, which only have light-sensitive R7/R8 photoreceptors, should also respond to field rotations. Indeed, *ninaE*^{8} flies also showed robust optomotor responses (Fig. 4B), consistent with efficient information transfer from R7/R8s to R6 cells (Fig. 3F). As predicted, the optomotor response was weakest with amber illumination when only single photoreceptor type (R8y), with only a small fraction of its spectral range being stimulated, drove on and off channels (amber motion), in agreement with intracellular recordings (Fig. 3I and fig. S5C).

We then asked whether R7/R8 inputs are necessary for motion detection. Flies in which R1–R6 photoreceptors expressed either Rh1-opsin (wild-type) or Rh3-opsin (UV) but had light-insensitive color (R7/R8) pathways attempted to follow visual motion (Fig. 4C). However, these torque responses were weaker than those of WT ($P = 0.012$) and UV flies ($P = 0.007$; also faster, $P = 0.0016$, two-way t test) (Fig. 4A), consistent with the briefer voltage responses of their R1–R6 and LMCs (Fig. 3A). Thus, R1–R6s inputs into motion pathway alone are sufficient for motion detection (*18, 20, 39, 40*), but R7 and R8 inputs boost the slow response components, adjusting the size, speed, and spectral range of optomotor behavior.

Next, to dissect the contribution of the different color channels in optomotor behavior, we rescued R8y, R8p, R7y, or R7p photoreceptors individually with a *norpA* WT transgene under control of their corresponding opsin promoters in blind norpA mutants (fig. S8, A to D). After verifying through patch-clamp recordings that R1–R6 photoreceptors of these flies were light-insensitive (fig. S8, E and F), we tested their optomotor behavior to black-and-white (spectrally broad) field rotations (Fig. 4, D and E). The strength of their optomotor responses reflected broadly the retinal distribution of opsins (*6, 15, 16*), supporting our hypothesis that motion perception emerges from spectral integration of receptor outputs. When R8y(Rh6)s, which reside in most ommatidia, were rescued, these populations alone provided a fly with robust motion perception (normalized mean torque response of 100%), whereas the responses of flies, with other R7/R8 subtypes rescued, were smaller ($P < 0.05$, $n = 10$ flies, two-way t test; fig. S11): for R7y(Rh4), 44.8%; R8p(Rh5), 32.5%; and R7p(Rh3), 40.2%. These differences may reflect variable amounts, distributions, or strengths of functional contacts, which different R7 and R8 types make with the motion pathway in the

lamina (28) and medulla circuits (*17, 24*). The sum of optomotor responses from these four opsin-rescued genotypes matched the mean response of ninaE^{8} flies (Fig. 4F), in which R7/R8 pairs are light-sensitive. Equally, the UV and ninaE^{8} flies responses to amber motion, although weak (Fig. 4, A and B right), were similar, highlighting the robustness of R7/R8 input for motion detection. Lastly, the sum of responses from flies with only light-sensitive R7/R8s (Fig. 4B) or only light-sensitive R1–R6s (Fig. 4C) approximated the mean response of WT flies (Fig. 4G). This unexpectedly linear summation allowed us to estimate the spectral range of motion vision by scaling the spectral sensitivity (nomogram) of each photo-receptor class by its apparent contribution to WT optomotor responses (Fig. 4H). The estimated range approximates the spectral sensitivity of WT LMCs (Fig. 4I), whereas the sensitivity of WT R1–R6s is more like their Rh1 input, suggesting that, from the first synapse onward, combined inputs from photoreceptors of different spectral classes mediate Drosophila's motion perception.

As a decisive test that R7/R8 inputs augment motion vision (Fig. 4J), we dimmed UV-lit field rotations to a level where UV flies' optomotor behavior nearly ceased and then shone additional amber light (595 nm), which is only detected by R8y photoreceptors, on the rotating field. Amber motion information strengthened the flies' torque responses, confirming that inputs from photo-receptors of different spectral sensitivities improve motion discrimination (Fig. 4, K and L).

Lastly, by using two-photon infrared microscopy to avoid stimulation of the photoreceptors, we imaged neural activity patterns in the motion-sensitive neurons (LPTCs) in the lobula plate of the Drosophila brain (figs. S12 to S14). The LPTCs of UV and WT flies were engineered to express genetically targeted calcium indicators (GCaMP3) that responded to changes in neural activity (fig. S12B). When such a fly viewed wide-field top-down and bottom-up movements of different colors, we found that individual LPTCs of both UV and WT flies preferred different motion directions (figs. S12, C and D; to S14). They responded to UV and amber-green image motions in comparable fashion; the responses to UV motion were stronger than those to amber motion [UV: DF/F (change in fluorescence/fluorescence) =70.5% ± 19.3; amber: 33.7% ± 21.2, ± SD, P =0.001, one-way ANOVA; n = 10 LPTCs from five UV flies].

We have shown that inputs from R7 and R8 photoreceptors converge with and shape R1–R6/LMC outputs, improving motion discrimination in *Drosophila*. These findings refute the longstanding hypothesis that motion detection in flies is mediated exclusively by one spectral class of photoreceptors (R1–R6) but agree with the circuit model, in which R7 and R8 photoreceptors feed information to R1–R6 terminals through gap-junctions (*28, 29*). Besides extending and equalizing the spectral range of motion detection so that each spectral band has more similar probability of being used, R7/R8 inputs adjust the sensitivity (size and speed) of optomotor responses. Sensitivity increases as each on and off channel receives inputs from eight superpositioned photo-receptors, instead of six as previously reported, with R7/R8 inputs adding extra low-frequency information about slow- or low-contrast changes. Nonetheless, R7/R8 inputs improve robustness of motion vision; by piggy-backing to the motion pathway just before the first visual synapse, inputs from even a single R7/R8 receptor class enable motion perception.

These results also suggest an answer to the old open question: Why are R7y/R8y and R7p/R8p pairs randomly distributed across the retina? Although a color-blind movement detector is in many senses optimal (41), it cannot respond to movement of two-color patterns if the intensities of the colors provide no contrast to the input channels: the isoluminant point (42). Furthermore, in the spatial domain, the receptive fields of on and off channels of an optimal motion detector should be maximally correlated, that is, identical, for the two channels to filter the scene in the same way (41). In a previous study (9), the capacity of many WT flies to respond to opposing movements of blue-green color contrast (of different intensity ratios) never fell to zero; thus, such flies showed no absolute point of perceptual isoluminance, consistent with our findings here. This suggests that Drosophila's motion-detection circuits may have evolved to minimize isoluminance effects by deriving its inputs from randomized combinations of spectral receptors, both within the same point in space and between neighboring points, to supply the on and off channels used for motion detection (*6, 15, 16*). Thus, these circuits provide simultaneous and robust encoding of multiple visual attributes from the ever-changing external world with limited wiring costs.

Supplementary Material

Refer to Web version on PubMed Central for supplementary material.

Acknowledgments:

We thank G. de Polavieja and people of the Juusola lab for discussions and I. Meinertzhagen and P. Gonzalez Bellido for assistance with electron microscopy. The work was supported by the Gatsby Charitable Foundation (GAT2839: M.J.), the open research fund of the State Key Laboratory of Cognitive Neuroscience and Learning (M.J. and S.T.), the Biotechnology and Biological Sciences Research Council grants (BB/H013849/1 and BB/F012071/1: M.J.)and (BB/G006865/1 and BB/D007585/1: R.C.H.), and the Intramural Research Program of Eunice Kennedy Shriver National Institute of Child Health and Human Development (HD008776–06: C.H.L.), the NSFC project (30810103906: S.T. and M.J.). The authors declare no competing financial interests. Supplementary materials accompany the paper on Science Online. Author contributions: Project initiation: M.J.; genetics: T.J.W., O.L., C.H.L., R.C.H., C.J.O'K., X.L.; electrophysiology:X.L., M.J., R.C.H., T.J.W.; behavior: S.D., M.M.C., T.J.W., M.J., S.T.; imaging: O.L., T.J.W., S.D., M.J.; electronmicroscopy: T.J.W.; immunohistochemistry: C.Y.T.; wrote the paper: M.J., with contributions from all authors.

References and Notes

1. Nishida S, Watanabe J, Kuriki I, Tokimoto T, Curr. Biol 17, 366 (2007). [PubMed: 17291762]
2. Takeuchi T, De Valois KK, Hardy JL, Vision Res. 43, 1159 (2003). [PubMed: 12705956]
3. Barlow HB, Behav. Brain Sci 24, 602 (2001). [PubMed: 12048943]
4. Knill DC, Pouget A, Trends Neurosci. 27, 712 (2004). [PubMed: 15541511]
5. Schiller PH, Proc. Natl. Acad. Sci. U.S.A 107, 17087 (2010). [PubMed: 20876118]
6. Hardie RC, J. Comp. Physiol. A 129, 19 (1979).
7. Cropper SJ, Wuerger SM, Behav. Cogn. Neurosci. Rev 4, 192 (2005). [PubMed: 16510893]
8. Gegenfurtner KR, Hawken MJ, Trends Neurosci. 19, 394 (1996). [PubMed: 8873357]
9. Yamaguchi S, Wolf R, Desplan C, Heisenberg M, Proc. Natl. Acad. Sci. U.S.A 105, 4910 (2008). [PubMed: 18353989]
10. Derrington AM, Curr. Biol 10, R268 (2000). [PubMed: 10753737]
11. Joesch M, Schnell B, Raghu SV, Reiff DF, Borst A, Nature 468, 300 (2010). [PubMed: 21068841]
12. Juusola M, Hardie RC, J. Gen. Physiol 117, 3 (2001). [PubMed: 11134228]
13. Zheng L et al., J. Gen. Physiol 127, 495 (2006). [PubMed: 16636201]

14. Chiappe ME, Seelig JD, Reiser MB, Jayaraman V, Curr. Biol 20, 1470 (2010). [PubMed: 20655222]
15. Britt SG, Feiler R, Kirschfeld K, Zuker CS, Neuron 11, 29 (1993). [PubMed: 8338666]
16. Chou WH et al., Neuron 17, 1101 (1996). [PubMed: 8982159]
17. Gao S et al., Neuron 60, 328 (2008). [PubMed: 18957224]
18. Rister J et al., Neuron 56, 155 (2007). [PubMed: 17920022]
19. Kaiser W, Liske E, J. Comp. Physiol 89, 391 (1974).
20. Heisenberg M, Buchner E, J. Comp. Physiol 117, 127 (1977).
21. O'Tousa JE et al., Cell 40, 839 (1985). [PubMed: 2985266]
22. Kirschfeld K, Franceschini N, Minke B, Nature 269, 386 (1977). [PubMed: 909585]
23. Hardie RC, Nature 339, 704 (1989). [PubMed: 2472552]
24. Takemura SY, Lu Z, Meinertzhagen IA, J. Comp. Neurol 509, 493 (2008). [PubMed: 18537121]
25. Bausenwein B, Wolf R, Heisenberg M, J. Neurogenet 3, 87 (1986). [PubMed: 3083074]
26. de Polavieja GG, Neural Comput. 18, 2102 (2006). [PubMed: 16846388]
27. Riehle A, Franceschini N, Exp. Brain Res 54, 390 (1984). [PubMed: 6723860]
28. Shaw SR, Fröhlich A, Meinertzhagen IA, Cell Tissue Res. 257, 295 (1989). [PubMed: 2776184]
29. Shaw SR, J. Exp. Biol 112, 225 (1984). [PubMed: 6392468]
30. Meinertzhagen IA, O'Neil SD, J. Comp. Neurol 305, 232 (1991). [PubMed: 1902848]
31. Scavarda NJ, O'tousa J, Pak WL, Proc. Natl. Acad. Sci. U.S.A 80, 4441 (1983). [PubMed: 16593338]
32. Feiler R et al., J. Neurosci 12, 3862 (1992). [PubMed: 1403087]
33. Kumar JP, Ready DF, Development 121, 4359 (1995). [PubMed: 8575336]
34. Gengs C et al., J. Biol. Chem 277, 42113 (2002). [PubMed: 12196539]
35. Liu CH et al., Neuron 59, 778 (2008). [PubMed: 18786361]
36. van Hateren JH, J. Comp. Physiol. A 158, 795 (1986). [PubMed: 3016255]
37. Juusola M, de Polavieja GG, J. Gen. Physiol 122, 191 (2003). [PubMed: 12860926]
38. Gonzalez-Bellido PT, Wardill TJ, Juusola M, Proc. Natl. Acad. Sci. U.S.A 108, 4224 (2011). [PubMed: 21368135]
39. Clark DA, Bursztyn L, Horowitz MA, Schnitzer MJ,Clandinin TR, Neuron 70, 1165 (2011). [PubMed: 21689602]
40. Eichner H, Joesch M, Schnell B, Reiff DF, Borst A, Neuron 70, 1155 (2011). [PubMed: 21689601]
41. Srinivasan MV, Vision Res. 25, 997 (1985). [PubMed: 4049749]
42. Kaiser W, in The Compound Eye and Vision of lnsects (Clarendon, Oxford, 1975), pp. 359–377.

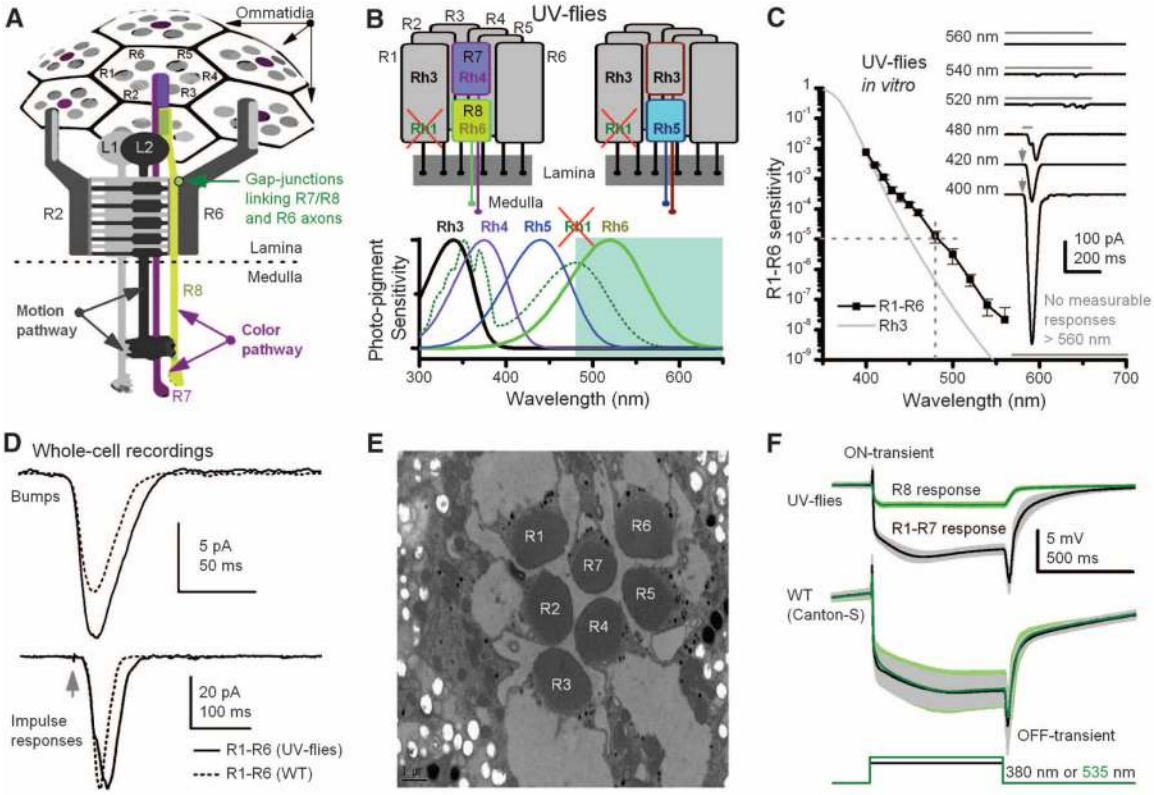

Fig. 1.

Manipulating spectral sensitivity of the motion pathway to elucidate circuit computations. (**A**)Schematic offly photo-receptors innervating motion and color pathways. A light point is sampled by six outer photoreceptors (R1–R6) in neighboring ommatidia and by central R7/R8 photoreceptors. These R1–R6s inner-vate LMCs (L1 and L2) in the first optic neuropile, lamina, whereas R7/R8 synapseinthesecondneuropile, medulla. Gap junctions link R7/R8 to R6 just before R1–R6 are brought together (superpositioned) for synaptic transmission (28). (**B**) In UV flies, UV-sensitive Rh3-opsin is expressed in R1–R6s, which contain nonfunctional Rh1-opsin (*ninaE*^{8}). This circumvents the spectral overlap between motion andR8pathways.(**C**)Spectral sensitivity of light-induced currents (inset) in dissociated R1–R6s of UV flies, diminishing <1/100,000 at ≥480 nm (mean ± SD; four photoreceptors). (Inset) Example responses to 2-ms flashes (arrows) or 50- or 500-ms stimuli (bars). (**D**) Although single-photon responses (bumps) can be larger than those of WT (Canton-S) and impulse responses last slightly longer, their responses are very similar to their WT counterparts, indicating normal-like phototransduction (fig. S4, A and B) (35). (**E**) Photoreceptors of UV flies have normal-like ultrastructure. (**F**) Electroretinograms (ERGs) show comparable dynamics to those of WT flies: Preferred colors evoke large receptor components and on and off transients, indicating normal synaptic transmission from R1–R6 to LMCs (means T SD; six flies). With UV flies, one can separate the responses for green (R8s) and UV (R1–R7s).

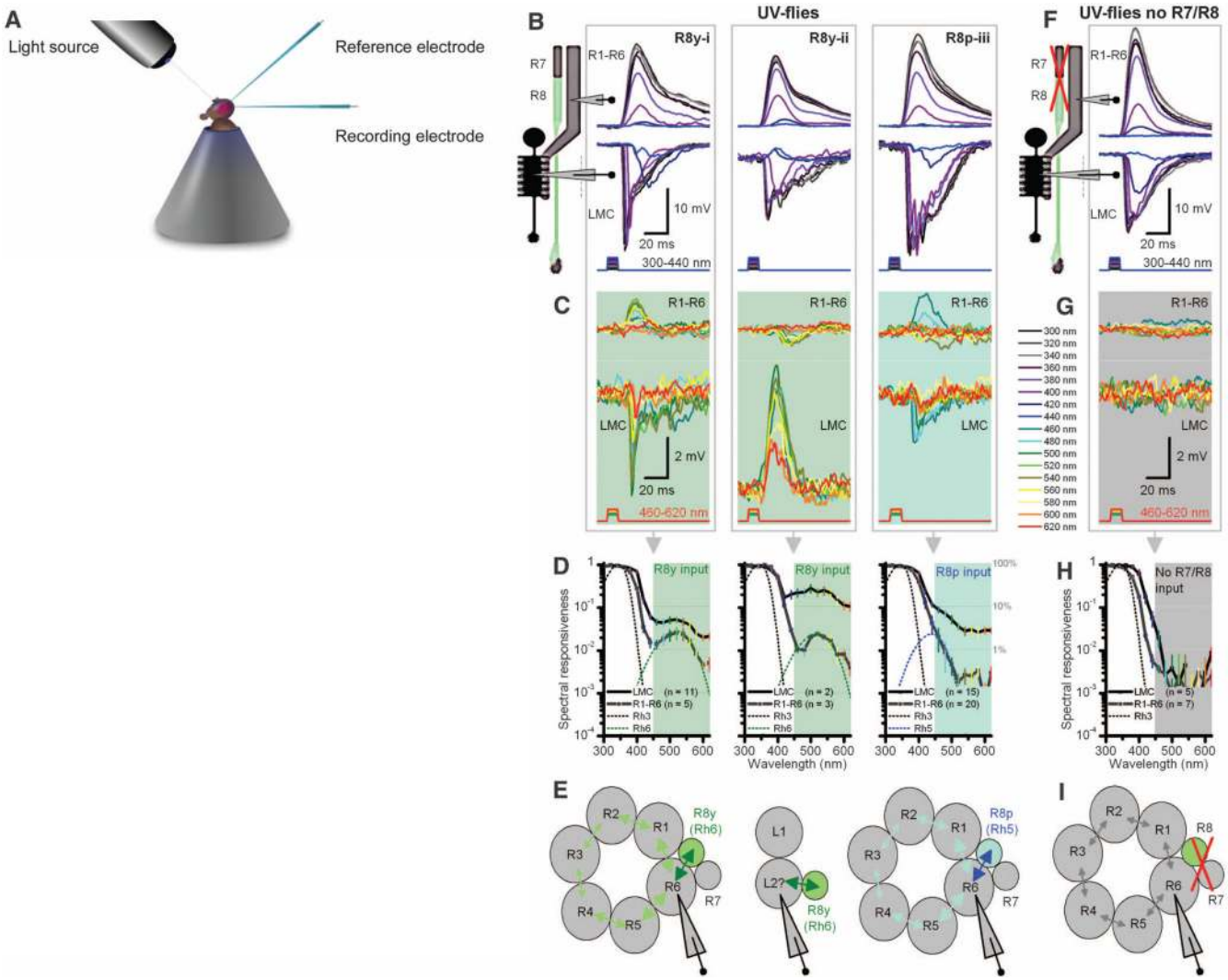

Fig. 2.

Motion pathway receives information from R8 photo-receptors in color pathway. (**A**) Schematic of in vivo recordings using monochromatic light. (**B**) Three intracellular response types from R1–R6 photoreceptors and postsynaptic LMCs to subsaturating short-wavelength (300 to 420 nm) pulses of equal energy. (**C**) Stimulating the same representative cells (B, i to iii) with equal long-wavelength (420 to 620 nm) pulses, which are undetectable by Rh3, reveals unexpected responses both in polarity and spectral responsiveness. (**D**) Spectral responsiveness of R1–R6 and LMC outputs confirms a second peak or bulge, which matches the sensitivity of R8y (Rh6) or R8p (Rh5) photoreceptors; right graph also includes cells with subtle long-wavelength range extensions. (E) Results suggest a model (29) in which information spreads via gap junctions from each R8 to R6 axon, and further to other photoreceptors in the same cartridge, before transmission to LMCs. Depolarizing responses (420 to 620 nm) in some LMCs suggest gap junctions between L2 and R8 axons. (**F**) In UV flies in which R1–R8 phototransduction was deactivated (*norpA*^{36}) and then rescued only in R1–R6 (i.e., light-insensitive R7/R8), R1–R6 and LMC have a sensitivity to short-wavelength stimuli that is similar to when R7/R8 are functional (B). (**G**) These R1–R6s and

LMCs cannot detect 460 to 620 nm. (**H**) Their spectral responsiveness matches the Rh3 sensitivity of dissociated cells (Fig. 1C). (**I**) With light-insensitive R7/R8s, information processing occurs independently within the motion pathway.

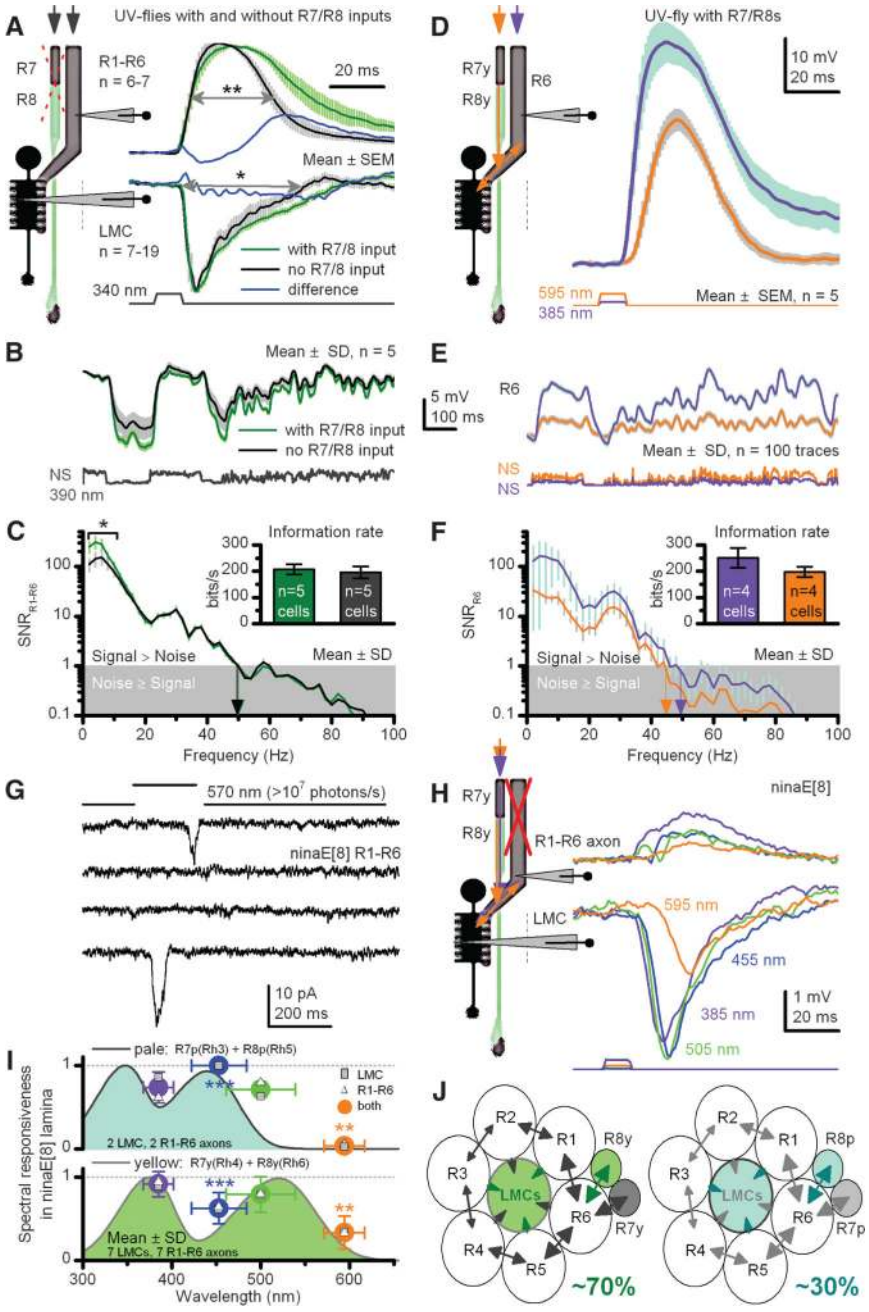

Fig. 3.

R7/R8 photoreceptors transmit information to a motion pathway shaping R1–R6 and LMC outputs. (**A**) Normalized R1–R6 and LMC outputs to a saturating UV impulse in UV flies with or without light-sensitive R7/R8s. Wider responses suggest extra R7 inputs. Differences highlight the change over time between the genotypes. (**B**) R1–R6 outputs to naturalistic UV-intensity series; NS, with or without light-sensitive R7/R8s. (**C**) Corresponding signal-to-noise ratios (SNRs) and information transfers (inset). (**D**) Apart from the three response types in Fig. 2C, ~10% of R1–R6s from UV flies also responded strongly (>25 mV) to amber, signifying direct R8y input to R6 (29) (figs. S6 and S7). (**E**) Responses to UV and

amber NS [different from (B)] in one presumptive R6. (**F**) High SNR with amber responses, containing ~70% of information of maximal UV responses (inset, three R6s). (**G**) Whole-cell recordings reveal that *ninaE*^{8} R1–R6s are profoundly light-insensitive (fig. S3B), lacking macroscopic light-induced current; ultrabright green-yellow light rarely evokes single-photon responses (two shown). (**H**) An in vivo example where presynaptic *ninaE*^{8} R1–R6 axon and postsynaptic LMC generate small responses, following R7/R8s' sensitivity, here R7y/R8y; similar recordings from nine LMCs and nine R1–R6s (fig. S5C). (**I**) Responsiveness of *ninaE*^{8} LMCs and R1–R6 axons track R7/R8-nomogram pairs. (**J**) Input to each lamina cartridge comes from R7, R8, R7y/R8y, or R7p/R8p pairs through gap junctions to R6 axons to drive synaptic output to LMCs. *P < 0.05; **P < 0.01, ***P < 0.005, one-way ANOVA.

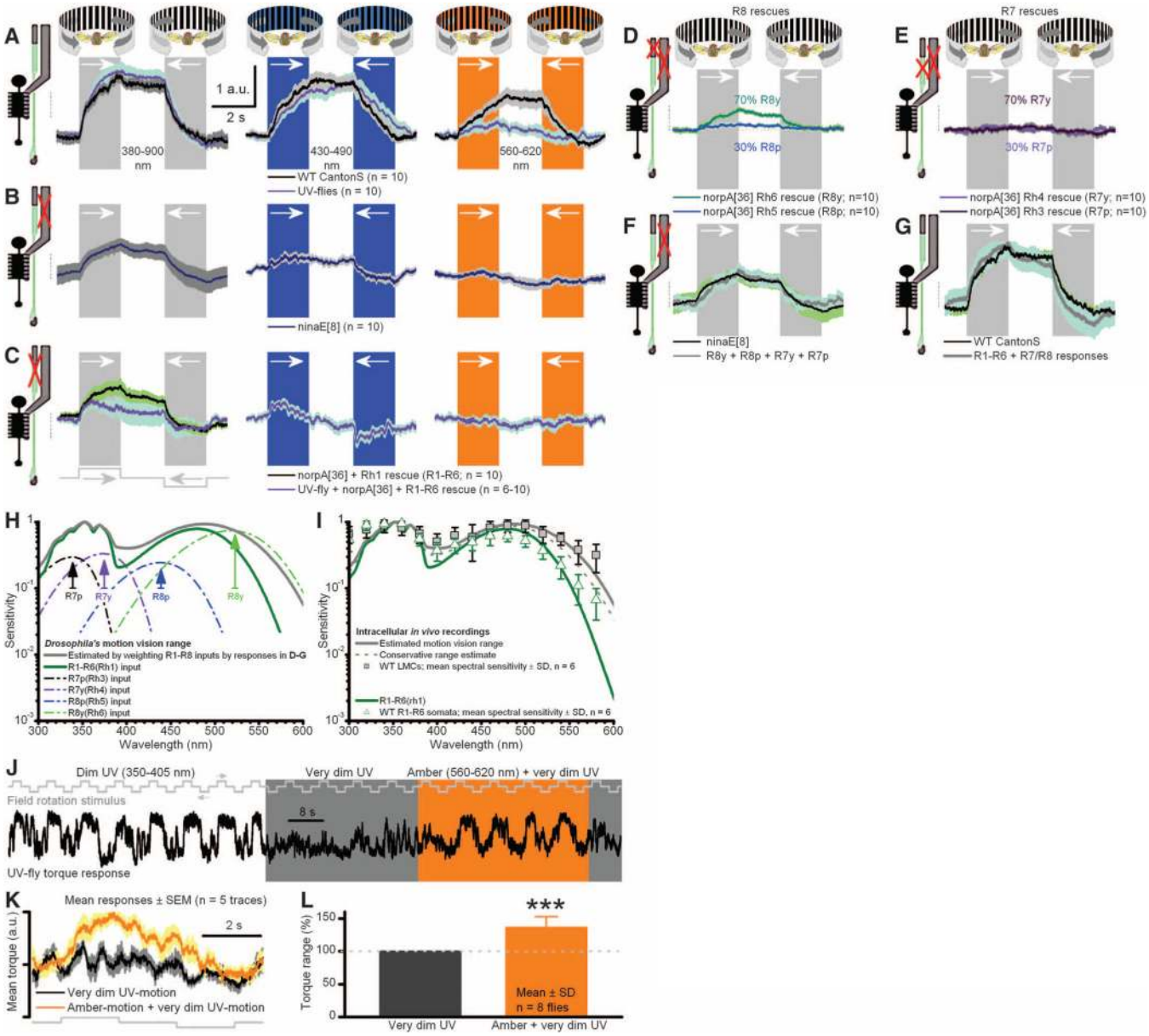

Fig. 4.

Signals from R1–R6 and R7/R8 sum to generate optomotor responses. Responses (yaw torque) of tethered flying Drosophila to different color-field rotations (black-white, black-blue, and black-amber) to left and right. (**A**) Both UV flies (R1–R6s expressing Rh3-opsin) and WT respond to broad spectral range of motions. a.u., arbitrary unit. (**B**) Mutant *ninaE*^{8}-flies, having light-insensitive R1–R6 photoreceptors (Fig. 3G; motion pathway) but normal R7/R8 photo-receptors, react to an equally broad spectral range of motions as in (A), but with weaker responses. (**C**) *norpA*^{36} flies, having R1–R6 photoreceptors rescued with Rh1 or Rh3 opsins, react to broad spectral range of motions but with weaker and faster responses than in (A). (**D**) Rescuing light sensitivity only in R8y or R8p photo-receptors enables visual motion perception. (**E**) Rescuing light sensitivity only in R7y or R7p photoreceptors enables weaker motion perception (fig. S11B). (**F**) Responses of *norpA*^{36} flies with rescued light

sensitivity in R7 and R8 photoreceptors equal the mean responses of *ninaE*^{8} flies. (**G**) Responses of *norpA*^{36} flies with rescued R1–R6 photoreceptors and *ninaE*^{8} flies (with normal R7/R8s) sum up the mean responses of WT flies. In (A) to (G), mean T SEM is shown in same scale. (**H**) Motion-vision range estimated by weighting R1–R8 inputs with their relative optomotor response strengths: (D) to (G). (**I**) Range coincides with LMCs' spectral sensitivity. (**J**) UV motion is dimmed until a fly's optomotor responses nearly cease. Adding amber light strengthens responses. (**K**) Corresponding averages. (**L**) R8y input improves motion discrimination by ~36% ($P = 0.0004$; t test for mean > 1).